

# Chapter 1

## Introduction

### 1.1. Fuel Production by Hydroprocessing

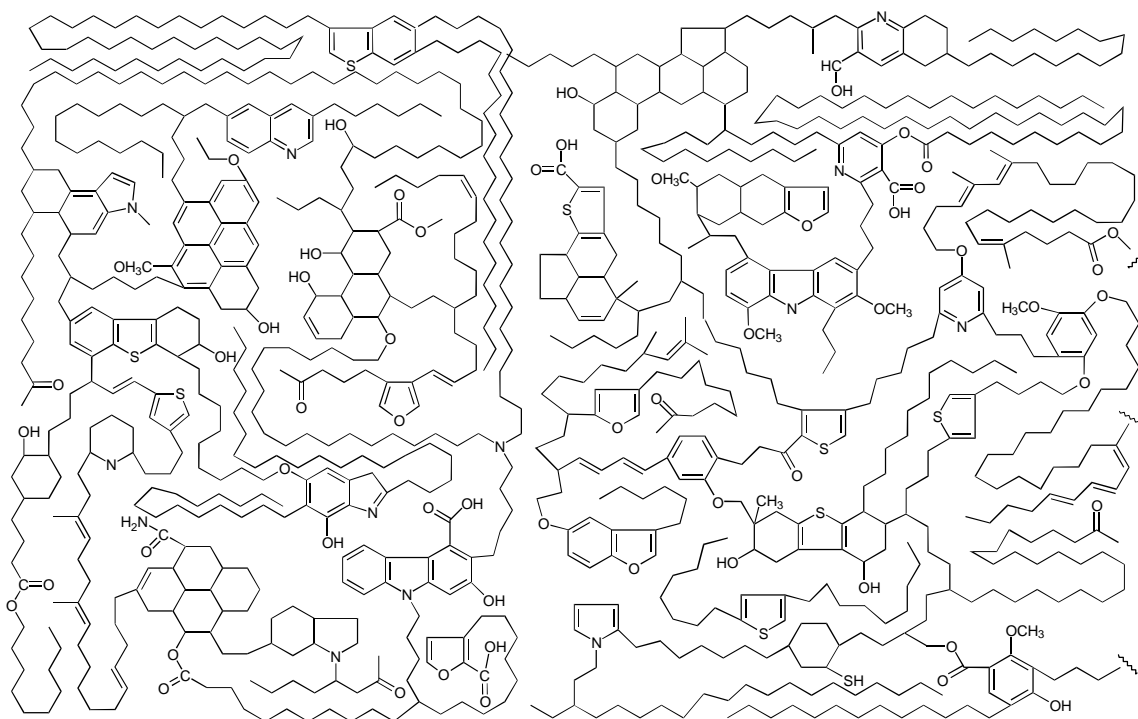
The processing of fossil feedstocks is becoming an increasingly important technology as high quality reserves dry up, and lower quality resources must be utilized. This effect is compounded by increasingly stringent regulations demanding lower sulfur levels in fuels used throughout the world. Recently enacted legislation demands that sulfur levels in diesel fuel be reduced from 500 ppm to 50 ppm by the year 2004 (1). Such high degrees of sulfur removal are known as deep hydrodesulfurization (hds). Among other things, such deep hds requires coincidental high levels of denitrogenation (hdn) because of the poisoning effect of nitrogen compounds on hds reactions. Nitrogen compounds in fuel liquids are also undesirable because they are corrosive, odorous, toxic, tend to polymerize and gel, and are poisons for acidic hydrocracking catalysts.

Hydroprocessing technology is not reserved to upgrading of petroleum cuts, but is applied to many hydrocarbon resources. These liquids include coal derived liquids (e.g. SRC – solvent refined coal) (2), liquids obtained from coliquefaction of waste tires with coal (3), shale-oil (bitumen) derived liquids (e.g. coker gasoil) (4, 5), agricultural oils (e.g. rapeseed, canola) (6), and waste animal fat (6). Furthermore, toxic organic waste may be dechlorinated, desulfurized, and denitrogenated using hydroprocessing technology (7). Petroleum based fuels have a high relative abundance of sulfur (8), while

coal and biologically derived liquids contain mostly oxygen impurities (9), and shale oils are typically rich in nitrogen (8). However, the essential treating processes and catalysts are similar in each case.

The complicated nature of the conversion processes can be exemplified by considering an example of a structural model for a heavy hydrocarbon resource, as shown in Figure 1.1 (10).

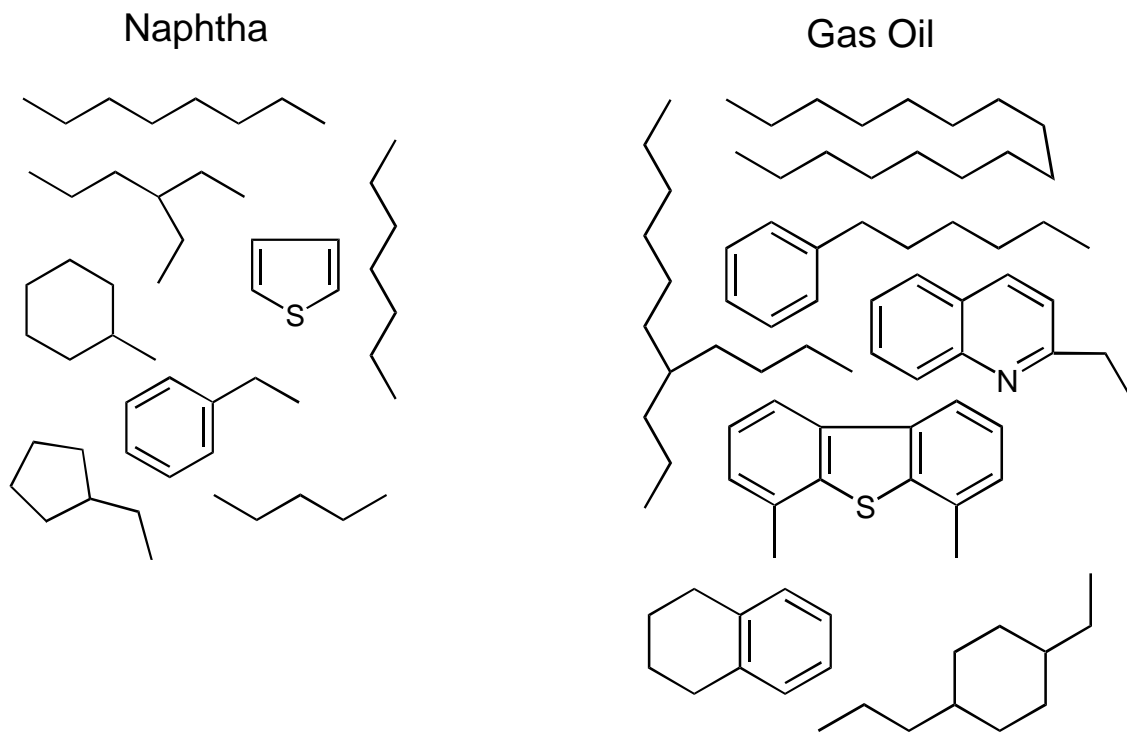
Figure 1.1: Adapted structural model of an oil shale molecule.



Large molecules such as these are variously known as shale oil, kerogen, or bitumen, and can vary greatly in structure depending on the source (11). In these structures, many nitrogen, sulfur and oxygen atoms are tied up in heterocyclic rings, while hydrocarbons are present as chains of aliphatics connecting aromatic structures. Hydroprocessing,

pyrolysis, and hydrocracking technologies are used to convert these heavy, impurity laden, fossil resources into fuel liquids consisting of mixtures of smaller molecules with favorable combustion properties and low impurity contents, as shown in Figure 1.2 (5). The aromatic heterocycles shown in Figure 1.2 are chemically stable and therefore persist in the processed liquids as target molecules for removal during subsequent upgrading steps.

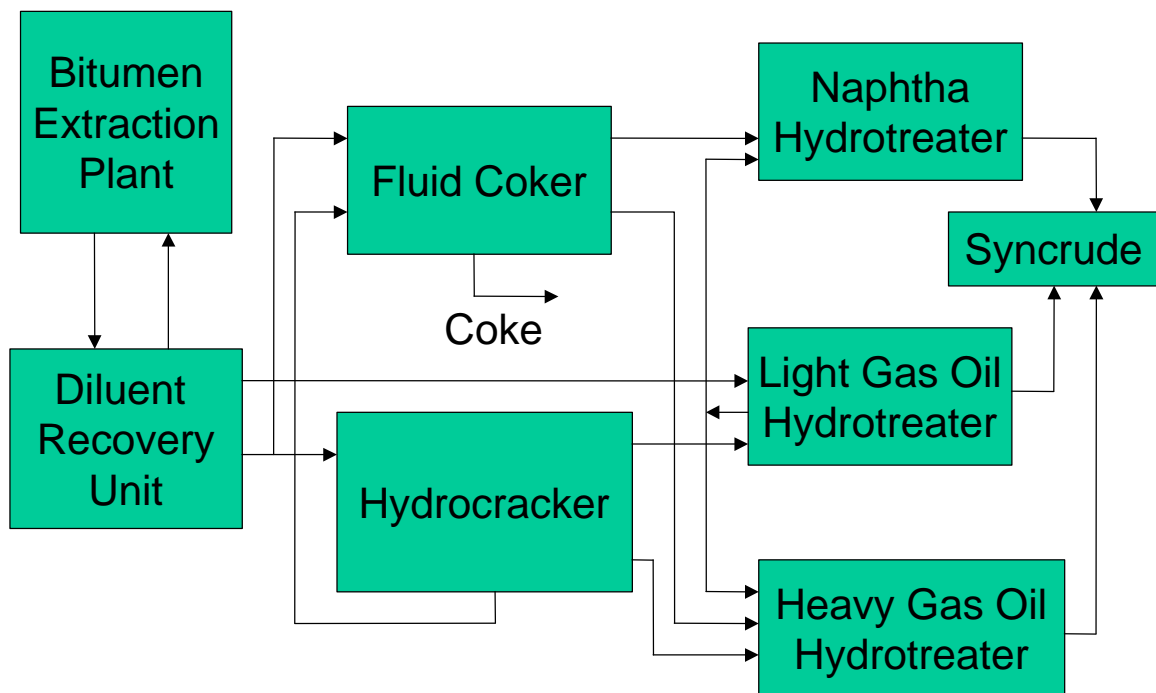
**Figure 1.2:** Structural models of naphtha and gas oil



An example of the simplified flowsheet of an industrial refining operation, which creates synthetic crude oil from oil-sand derived bitumen, is shown in Figure 1.3. Here the bitumen is extracted from its source in a solvent. The solvent is recovered, and the

bitumen exposed to a coker or hydrocracker. The products of these processes are either recycled or hydroprocessed. The recovered liquids from hydroprocessing are then recombined to form the synthetic crude oil product. The overall process also requires a hydrogen plant, to generate hydrogen from natural gas for the hydroprocessing operations, and a sulfur recovery plant, to recover the hydrogen sulfide produced in the refining operations.

**Figure 1.3:** Production of synthetic crude oil from bitumen



Many factors contribute to the choice of hydrotreating catalyst used in a given process. CoMoS/Al<sub>2</sub>O<sub>3</sub> catalysts are typically used for hydrodesulfurization reactions, NiMoS/Al<sub>2</sub>O<sub>3</sub> is used in hydrodenitrogenation (due to its higher hydrogenation activity),

and NiWS/Al<sub>2</sub>O<sub>3</sub> is favored for situations where aromatics saturation is desired in the presence of substantial amounts of heteroatoms (12). Petroleum resids and other heavier resources frequently contain metals such as Ni and V, which can deposit on catalysts as sulfides. These Ni and V sulfides tend to deactivate the catalyst by clogging the catalyst pores. Thus the catalytic reactors which perform hydrodemetallation tend to have moving bed technologies with continual catalyst replacement and recovery, and the demetallation catalysts themselves have large pores (and low loadings of active component) to accommodate the sulfide deposition (13).

Hydrodenitrogenation has received relatively less attention in the literature than hydrodesulfurization, but has been investigated intensively since the oil crisis of 1974. Several reviews are available regarding the hydrodenitrogenation process (4, 8, 14, 15, 16, 17, 18), summarizing the past and present state-of-affairs.

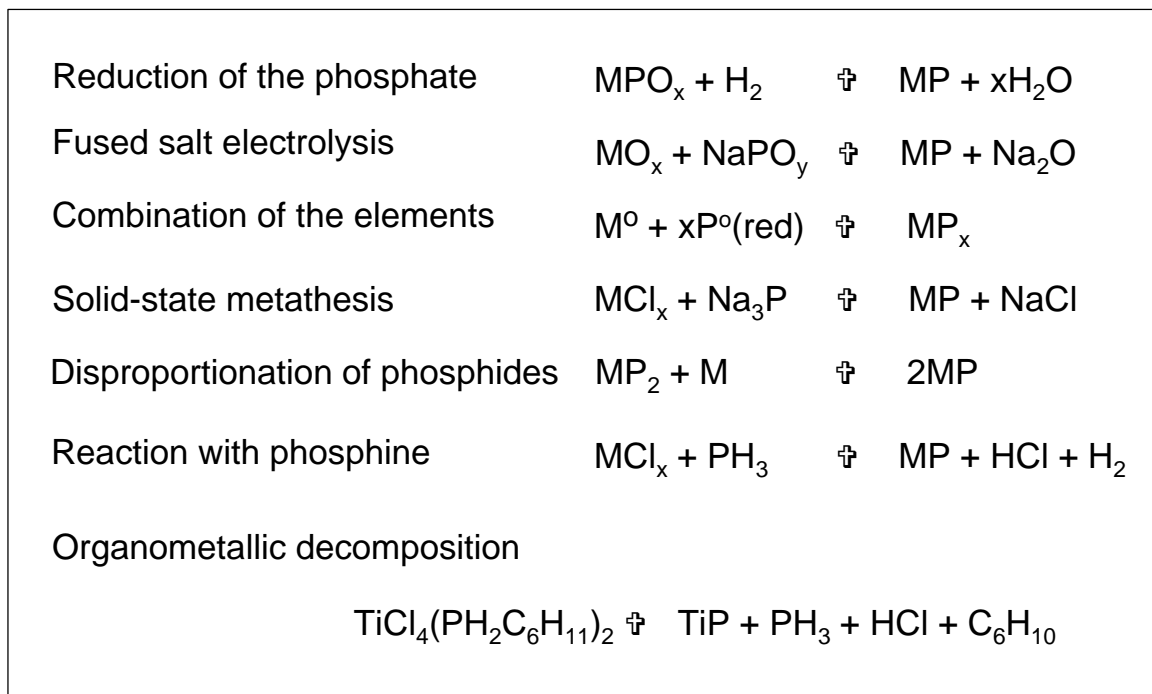
## **1.2. Introduction to Transition Metal Phosphides**

The catalysts investigated in this study comprise an undeveloped class of transition metal catalysts, the transition metal phosphides. Attention is focussed on the monophosphides of molybdenum and tungsten, because they are the most important elements in standard sulfide catalysts and they readily form monophosphides which are stable in the hydroprocessing conditions. The preparation and properties of transition metal phosphides have been reviewed in several publications (19, 20, 21, 22).

Many techniques have been applied to the preparation of transition metal phosphides, including combination of the elements (23, 24, 25, 26, 27), disproportionation of

phosphides (28, 29), metathesis (30, 31, 32, 33), fused salt electrolysis (26, 34), hydrogen reduction of phosphates (35, 36, 37, 38, 39, 40), chemical vapor deposition of organometallic precursors (41), and reactions with phosphine (27). Figure 1.4 summarizes the generalized reactions involved with these processes.

**Figure 1.4:** Preparation methods of transition metal phosphides

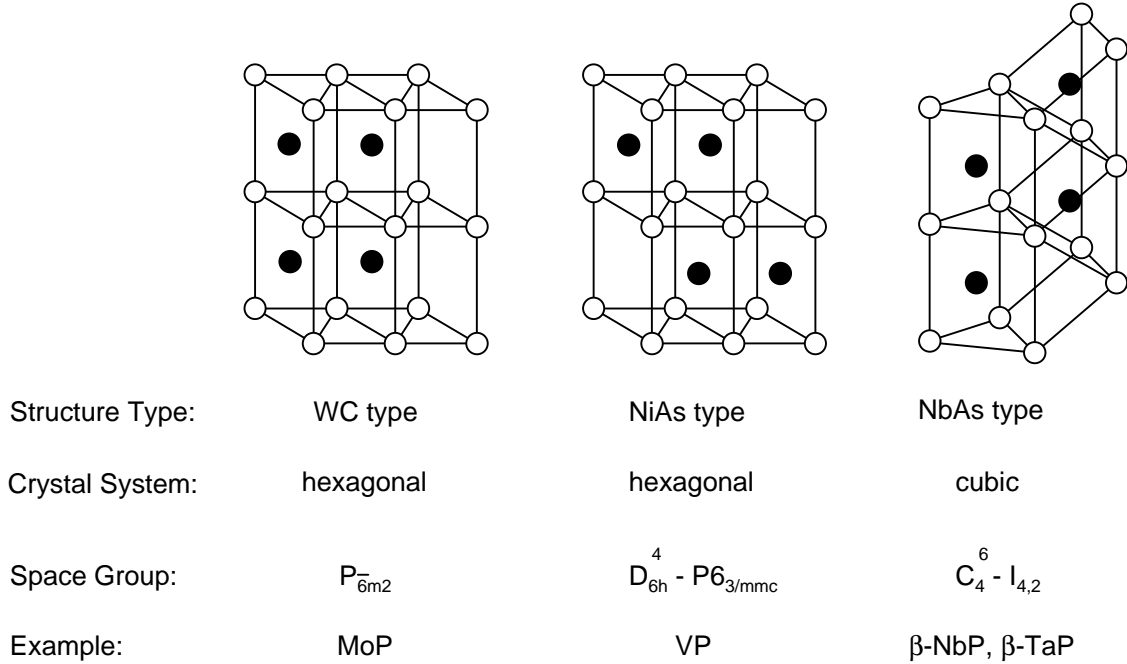


Trends in the crystal structures and properties of the first row transition metal monophosphides are shown in Table 1.1. The crystal structures range, from left to right on the periodic table, from the simple rocksalt type structure with ionic characteristics, to orthorhombic structures with metallic character. The XPS binding energy shifts also

**Table 1.1.** Structural trends in the first row transition metal monophosphides

|                          | ScP        | TiP                  | VP                   | CrP, MnP, FeP, CoP                    | NiP          |
|--------------------------|------------|----------------------|----------------------|---------------------------------------|--------------|
| Group                    | IIIA       | IVA                  | VA                   | VIA, VIIA, VIII, VIII                 | VIII         |
| Structure Type           | NaCl       | TiP                  | NiAs                 | MnP                                   | NiP          |
| Crystal System           | cubic      | hexagonal            | hexagonal            | orthorhombic                          | orthorhombic |
| Nature                   | ionic      | semiconductor        | metallic             | increasing metallic character $\zeta$ |              |
| P - coordination         | octahedral | $\Omega$ mix $\zeta$ | triangular prismatic | chains                                | pairs        |
| M - coordination         | octahedral | octahedral           | octahedral           | chains                                | pairs        |
| P - binding energy shift | 2.2        | 1.5                  | 0.8                  | - , 0.5, 0.4, -                       | -            |
| M - binding energy shift | 1.1        | 0.5                  | 0.0                  | - , 0.1, 0.2, -                       | -            |
| shortest P – M distance  | 2.66       | 2.48                 | 2.41                 | 2.38, 2.36, 2.31, 2.30                | -            |
| shortest M – M distance  | 3.76       | 2.91                 | 3.16                 | 2.89, 2.89, 2.85, 2.88                | -            |
| shortest P – P distance  | 3.76       | 3.50                 | 3.39                 | 3.38, 3.43, 3.35, 3.33                | -            |

**Figure 1.5:** Structural types of transition metal monophosphides



decrease with position on the periodic table, and are near elemental values in the majority of cases, consistent with the electrical properties noted above.

Overall, the crystal chemistry of the metallic phosphides considered in this study is dominated by structures of triangular prismatic units of phosphorus surrounding each metal atom. A diagram of the common structure types based on triangular prismatic units is provided in Figure 1.5.

Many monophosphides, including WP, CrP, MnP, FeP, and CoP, adopt the orthorhombic MnP type structure. The MnP structure is obtained by lattice distortions which break the symmetry within the (001) plane from hexagonal to rhombic. The lattice distortion effectively doubles the a lattice parameter, while retaining the b and c dimensions (42). The transition between the NiAs and MnP structure types is thought to lead to heightened metallic character (42, 43). Compounds are known which have the

NiAs structure at room temperature, while transforming into the MnP type structure at elevated temperature (the sulfide VS is an example). The extent of distortion increases smoothly with temperature (43).

The crystal chemistry of phosphides is intermediate between that of interstitial compounds, i.e. the nitrides and carbides, and layered hexagonal sulfides. In general, in the related Mo and W carbides and nitrides, the carbon and nitrogen atoms reside in interstitial sites found in metal lattices, thus they have close packed metal structures. Because the larger P atoms do not fit within the interstitial sites, their incorporation into the metal framework expands the metal lattices, and results in different crystal forms.

Table 1.2 reports the bulk density, the specific volume per metal atom, and the average metal-metal shortest distance, for the most relevant Mo and W compounds. The densities were found in the literature (44), the specific volume per metal atom was calculated as the molecular weight divided by the density, and the average shortest metal-metal bond distance is taken to be the average diameter of a metal atom, calculated as the cube root of the specific volume.

Molybdenum and tungsten disulphides, MoS<sub>2</sub> and WS<sub>2</sub>, form layered structures having a van der Waals gap between hexagonal layers. As a result of the saturated bonding along the basal plane, the catalytic sites of layered disulfides are thought to be located along the crystallite edges, and not along the basal plane.

Table 1.3 summarizes the lattice parameters for a number of compounds relevant to this study (43, 45). The parameter *s*, also tabulated in Table 1.3, is the number of hexagonal layers stacked in the *c* direction per unit cell. These values were collected from structural diagrams found in the literature (19, 46). The interlayer distance is

**Table 1.2:** Densities and volumetric characteristics of molybdenum and tungsten compounds relevant to this study.

| Mo compounds          | units                              | Mo    | Mo <sub>2</sub> N | Mo <sub>2</sub> C | MoP   | MoS <sub>2</sub> |
|-----------------------|------------------------------------|-------|-------------------|-------------------|-------|------------------|
| mol. wt. (per m)      | g mol <sup>-1</sup>                | 96    | 103               | 102               | 127   | 160              |
| density               | g cm <sup>-3</sup>                 | 10.2  | 9.4               | 8.9               | 6.2   | 4.8              |
| specific metal volume | nm <sup>3</sup> atom <sup>-1</sup> | 0.016 | 0.018             | 0.019             | 0.034 | 0.055            |
| average m-m distance  | nm                                 | 0.25  | 0.26              | 0.27              | 0.32  | 0.38             |
| W compounds           | units                              | W     | W <sub>2</sub> N  | WC                | WP    | WS <sub>2</sub>  |
| mol. wt. (per m)      | g mol <sup>-1</sup>                | 184   | 191               | 196               | 215   | 248              |
| density               | g cm <sup>-3</sup>                 | 19.4  | 17.8              | 15.6              | 8.5   | 7.5              |
| specific metal volume | nm <sup>3</sup> atom <sup>-1</sup> | 0.016 | 0.018             | 0.021             | 0.042 | 0.055            |
| average m-m distance  | nm                                 | 0.25  | 0.26              | 0.28              | 0.35  | 0.38             |

defined here as the lattice parameter  $c$  divided by  $s$ . The interlayer distance is a quantitative estimate of the m-m bond distance in the  $c$  direction. A parameter  $r$ , the interlayer distance ratio, can be defined as the interlayer distance divided by the lattice parameter  $a$ . The interlayer distance ratio  $r$  is a measure of the relative m-m distances in the  $c$  direction to the m-m distance in the  $a, b$  plane. The values in Table 1.3 demonstrate the basic principle that the interlayer distance ratios are much greater than unity for the layered materials. In contrast, for the materials such as the hexagonal carbides, nitrides, and phosphides with NiAs and WC structures noted in Figure 1.4, the  $r$  values are close to, or less than, unity. Similarly, as was noted previously, the lattice distortion creating MnP from the NiAs structure effectively doubles the lattice parameter  $a$ . Therefore, the in-plane parameter is taken to be the average of  $b$  and  $a/2$  for materials with this structure

**Table 1.3:** Structural parameters of materials adopting the WC, NiAs, MnP, and layered hexagonal structure types.

| WC structure type                      | a    | b    | c    | s | $r = (c/s)/a$           |
|--|------|------|------|---|-------------------------|
| WC                                     | 2.91 | -    | 2.84 | 1 | 0.98                    |
| MoP                                    | 3.22 | -    | 3.19 | 1 | 0.99                    |
| $\delta$ -TaN                          | 2.94 | -    | 2.87 | 1 | 0.98                    |
| HfS                                    | 3.38 | -    | 3.44 | 1 | 1.02                    |
| NiAs structure type                    | a    | b    | c    | s | $r = (c/s)/a$           |
| NiAs                                   | 3.61 | -    | 5.02 | 2 | 0.70                    |
| VP                                     | 3.18 | -    | 6.22 | 2 | 0.98                    |
| TiS                                    | 3.32 | -    | 6.38 | 2 | 0.96                    |
| VS                                     | 3.32 | -    | 5.84 | 2 | 0.88                    |
| CoS                                    | 3.37 | -    | 5.18 | 2 | 0.77                    |
| MnP structure type                     | a    | b    | c    | s | $r = (c/s)/((a/2+b)/2)$ |
| MnP                                    | 5.26 | 3.17 | 5.92 | 2 | 1.02                    |
| WP                                     | 5.73 | 3.25 | 6.22 | 2 | 1.02                    |
| CrP                                    | 5.36 | 3.11 | 6.02 | 2 | 1.04                    |
| FeP                                    | 5.19 | 3.10 | 5.79 | 2 | 1.02                    |
| RuP                                    | 5.52 | 3.17 | 6.12 | 2 | 1.03                    |
| VS                                     | 5.87 | 3.30 | 5.82 | 2 | 0.93                    |
| NbS                                    | 6.39 | 3.33 | 5.87 | 2 | 0.90                    |
| Well known layered hexagonal materials | a    | b    | c    | s | $r = (c/s)/a$           |
| MoS <sub>2</sub>                       | 3.16 | -    | 12.3 | 2 | 1.95                    |
| WS <sub>2</sub>                        | 3.11 | -    | 12.4 | 2 | 1.99                    |
| C – graphite                           | 2.46 | -    | 6.70 | 2 | 1.36                    |
| BN – hexagonal                         | 2.50 | -    | 6.66 | 2 | 1.33                    |

type. The interlayer distance ratios  $r$  calculated for the MnP type structures are also found to be close to unity.

It should be concluded that atoms located along the  $a, b$  plane in MoP and WP are not coordinatively saturated, as found in the layered MoS<sub>2</sub> and WS<sub>2</sub> structures, making these atoms available for catalytic function. This represents a fundamental difference in the nature of phosphides, carbides, and nitrides compared to the well studied disulfide materials.

### 1.3. Organization of Thesis

This dissertation reports the development and application of a new class of hydroprocessing catalysts, the transition metal phosphides. Specifically, MoP and WP catalysts were identified and investigated for their catalytic properties. These compounds were prepared in bulk form, and supported on moderate surface area ( $\sim 90 \text{ m}^2 \text{ g}^{-1}$ ) alumina and silica supports. The mechanism of hydrodenitrogenation reactions on the silica supported phosphides was investigated by comparing the reactivities of a group of amines including *n*-pentylamine, *tert*-pentylamine, *neo*-pentylamine, piperidine, and pyridine.

The remainder of this dissertation is organized as follows:

Chapter 2 reports the synthesis of bulk WP and its application to the hydroprocessing (hydrodenitrogenation and hydrodesulfurization) of a model oil. The tungsten phosphide was found to be an effective hydroprocessing catalyst, superior to any other tungsten

compound tested under the same conditions, and was comparable in activity to a commercial hydroprocessing catalyst.

Chapter 3 presents the synthesis and activity of molybdenum phosphide supported on  $\gamma$ -alumina. These materials were also effective hydroprocessing catalysts. EXAFS characterization of a 7 wt% MoP/ $\gamma$ -Al<sub>2</sub>O<sub>3</sub> catalyst revealed that highly dispersed phosphides exist on the surface of these materials. This was corroborated by analysis of the chemisorption characteristics of the materials.

Chapter 4 reviews the reactions observed during hydroprocessing of simple N, S, and O containing molecules.

Chapter 5 presents the synthesis and activity of silica supported phosphides. This chapter also contains the results of a HDN mechanism study, in which comparison of the reactivities of *n*-pentylamine, *tert*-pentylamine, and *neo*-pentylamine result confirmed the dominance of a bimolecular elimination mechanism in hydrodenitrogenation over the phosphides.

Chapter 6 presents the results of the pyridine and piperidine hydrodenitrogenation experiments, and the application of kinetic analysis to the results of each. Piperidine was found to decompose by a second order process, while pyridine was found to react according to zeroth order disappearance of the hydrogenated intermediate piperidine.

## References

1. Mester, Z. C., Trends in diesel fuel sulfur regulations *Preprints: Am. Chem. Soc. Div. Pet. Chem.* **44** 681 (2000).
2. Curtis, C. W., and Pellegrino, J. L., Activity and selectivity of molybdenum catalysts in coal liquefaction reactions *Preprints: Am. Chem. Soc. Div. Fuel Chem.* **33**(1), 376 (1988).
3. Sharma, R. K., Zondlo, J. W., and Dadyburjor, D. B., A kinetic scheme for catalytic coliquefaction of coal and waste tire *Energy and Fuels* **12**, 589 (1998).
4. Gray, M. R., Composition and hydrotreating of bitumen and heavy oil-derived ditillates *AOSTRA J. Res.* **6**, 185 (1990).
5. Yui, S., The role of catalysts in Syncrude's operation *Can. Chem. News* **51**(7), 25 (1999).
6. Stumborg, M., Wong, A., and Hogan, E., Hydroprocessed vegetable oils for diesel fuel improvement in "Liquid Fuels, Lubricants, and Additives from Biomass", p. 157, American Society of Agricultural Engineers, St. Joseph, MI (1994).
7. Gioia, F., and Murena, F., Simultaneous catalytic hydroprocessing of chlorine-, nitrogen-, and sulfur-containing aromatic compounds *J. Haz. Mat.* **57**, 177 (1998).
8. Schulz, H., Schon, M., and Rahman, N., Hydrogenative denitrogenation of model compounds as related to the refining of liquid fuels *Stud. Surf. Sci. Catal.* **27**, 201 (1986).
9. Maggi, R., and Delmon, B., A review of catalytic hydrotreating processes for the upgrading of liquids produced by flash pyrolysis *Stud. Surf. Sci. Catal.* **106**, 99 (1997).
10. Freund, H., Application of a detailed chemical kinetic model to kerogen maturation *Energy and Fuels* **6**, 318 (1992).
11. Speight, J. G., "The Chemistry and Technology of Petroleum 2<sup>nd</sup> Ed." Marcel Dekker, NY (1991).
12. "Master Product List for Refinery and Petrochemical Processing" Criterion Catalyst Company, Houston, TX (2000).
13. Moyses, B. M., Hydroprocessing of heavy oils *Chem. Econ. Eng. Rev.* **14**(10), 10 (1982).
14. Girgis, M. J., and Gates, B. C., Reactivities, reaction networks, and kinetics in high-pressure catalytic hydroprocessing *Ind. Eng. Chem. Res.* **30**, 2021 (1991).
15. Katzer, J. R., and Sivasubramanian, R., Process and Catalyst Needs for Hydrodenitrogenation *Catal. Rev.- Sci. Engr.* **20**(2), 155-208 (1979)
16. Ho, T., Hydrodenitrogenation Catalysis *Catal. Rev.-Sci. Eng.* **30**(1), 117-160 (1988)
17. Minderhoud, J. K., and van Veen, J. A. R., First-stage hydrocracking: Process and catalytic aspects *Fuel Proc. Tech.* **35**, 87 (1993).
18. Prins, R., Jian, M., Flechsenhar, M., Mechanism and kinetics of hydrodenitrogenation *Polyhedron* **16**(18), 3235 (1997).
19. Aronsson, B., Lundström, T., and Rundqvist, S., "Borides, Silicides and Phosphides" John Wiley and Sons, London, U.K. (1965).
20. Toy, A. D. F., Phosphorus, in "Comprehensive Inorganic Chemistry" Chapter 20 (Bailar, J. C., Emeléus, H. J., Nyholm, R., and Trotman-Dickenson, A. F., Eds.) Pergamon Press, Oxford, UK (1973).
21. Corbridge, D. E. C., "Phosphorus: Studies in Inorganic Chemistry" Vol. 10, p. 71 Elsevier Press (1990).
22. Corbridge, D. E. C., Pearson, M. S., and Walling, C., "Topics in Phosphorus Chemistry" Vol. 3, p.123 John Wiley and Sons, NY (1966).
23. Rundqvist, S., New metal-rich phosphides of niobium, tantalum, and tungsten *Nature* **211**(5051), 847 (1966).
24. Rundqvist, S., The crystal structure of Mo<sub>4</sub>P<sub>3</sub> *Acta Chem. Scand.* **19**, 393 (1965).
25. Rundqvist, S., and Lundström, T., X-ray studies of molybdenum and tungsten phosphides *Acta Chem. Scand.* **17**, 37 (1963).
26. Lewis, G. and Myers, C. Vaporization properties of iron phosphides **67**, 1289 (1963)
27. Schönberg, N., An x-ray investigation of transition metal phosphides *Acta Chem. Scand.* **8**, 226 (1954).
28. Fjellvåg, H., Kjekshus, A., and Andresen, A. F., Magnetic and structural properties of transition metal substituted MnP. III. Mn<sub>1-t</sub>Fe<sub>t</sub>P (0.00≤t≤0.30) *Acta Chem. Scand. A* **38**, 711 (1984).

- 
29. Fjellvåg, H., and Kjekshus, A., Magnetic and structural properties of transition metal substituted MnP. IV.  $Mn_{1-x}Ni_xP$  *Acta Chem. Scand. A* **38**, 719 (1984).
  30. Ripley, R. I., The preparation and properties of some transition metal phosphides *J. Less-Common Met.* **4**, 496 (1962).
  31. Hector, A. L., and Parkin, I. P., Room-temperature-initiated routes to titanium and vanadium pnictides *Inorg. Chem.* **33**, 1727 (1994).
  32. Rowley, A. T., and Parkin, I. P., Convenient synthesis of lanthanide and mixed lanthanide phosphides by solid-state routes involving sodium phosphide *J. Mater. Chem.* **3**(7), 689 (1993).
  33. Hector, A. L., and Parkin, I. P., Self-propagating routes to transition-metal phosphides *J. Mater. Chem.* **4**(2), 279 (1994).
  34. Gingerich, K. A., Vaporization behavior and phosphorus decomposition pressures of tungsten monophosphide *J. Phys. Chem.* **68**(4), 768 (1964).
  35. Li, W., Dhandapani, B., and Oyama, S. T., Molybdenum phosphide: A novel catalyst for hydrodenitrogenation *Chem. Lett.* 207 (1998).
  36. Rose, H. *Pogg. Ann.* **24**, 232 (1832).
  37. Ephraim, F., and Rossetti, C., *Helv. Chim. Acta* **12**, 1025 (1929).
  38. Sweeny, N. P., Rohrer, C. S., and Brown, O. W., Dinickel phosphide as a heterogeneous catalyst for the vapor phase reduction of nitrobenzene with hydrogen to aniline and water **80**, 799 (1958).
  39. Nozaki, F., and Adachi, R., Chemical composition of the catalyst prepared by reduction of nickel orthophosphate in hydrogen and catalytic activity for partial hydrogenation of 1,3-butadiene *J. Catal.* **40**, 166 (1975).
  40. Gopalakrishnan, J., Pandey, S., and Rangan, K. K., Convenient route for the synthesis of transition-metal pnictides by direct reduction of phosphate, arsenate, and antimonate precursors *Chem Mater.* **9**, 2113 (1997).
  41. Lewkebandara, T. S., Proscia, J. W., Winter, C. H., Precursor for the low-temperature deposition of titanium phosphide films *Chem. Mater.* **7**, 1053 (1995).
  42. Tremel, W., Hoffmann, R., and Silvestre, J., Transition between NiAs and MnP type phases: an electronically driven distortion of triangular ( $3^6$ ) nets *J. Am. Chem. Soc.* **108**, 5174 (1986).
  43. Franzen, H. F., Structure and bonding in metal-rich compounds: pnictides, chalcides and halides *Prog. Sol. St. Chem.* **12**, 1 (1978).
  44. CRC Handbook of Chemistry and Physics 66<sup>th</sup> edition, Weast, R. C., Astle, M. J., and Beyer, W. H., Eds. p. B-68, CRC Press, Boca Raton, FL (1986).
  45. Powder Diffraction Files, J.C.P.D.S.-I.C.D.D., Pittsburgh, PA (1992).
  46. Comprehensive Inorganic Chemistry, Bailar, J. C., Jr., Emeleus, H. J., Nyholm, R., and Trotman-Dickenson, A. F., Eds. Pergamon Press, Oxford (1973).